MULTISCALE FOURTH-ORDER MODELS FOR IMAGE RESTORATION, INPAINTING AND LOW-DIMENSIONAL SETS RECOVERY

Zakaria Belhachmi, Moez Kallel, Maher Moakher, Anis Theljani

MULTISCALE FOURTH-ORDER MODELS FOR IMAGE RESTORATION, INPAINTING AND LOW-DIMENSIONAL SETS RECOVERY

ZAKARIA BELHACHMI*, MOEZ KALLEL†, MAHER MOAKHER‡, AND ANIS THELJANI§

Abstract. We consider a fourth-order variational model for solving image inpainting and restoration problems, with emphasis on the recovery of low-order sets (edges, corners) and the curvature. The approach consists of constructing a family of regularized functionals and to select, locally and in an adaptive way, the regularization parameters which control the diffusion of the reconstruction operator. Unlike the usual methods which optimize the parameters a priori and lead, in general, to complex systems of PDEs, our approach is based on a continuous, linear, high-order diffusion model dynamically adjusted at the discrete level. We analyze the method in the framework of the calculus of variations and with the Γ-convergence tools and we show that it yields results that might be expected from more complex systems of PDEs. We obtain simple discrete algorithms based on mixed finite elements. We also consider a new model which couples second and fourth order derivatives, in analogy with the Euler's elastica functional and we show that our simple model performs as well. We present several numerical examples to test our approach and to make some comparisons with existing methods.

Key words. Image inpainting - Inverse problems - Regularization procedures - Mixed finite elements.

AMS subject classifications. 65M32 - 65M50 - 65M22- 94A08 - 65N22 - 35G15- 35Q68

1. Introduction. Digital image inpainting started with the works of engineers and computer scientists in the mid-nineties of last century. It refers to restoring a damaged image with missing information. This type of image processing task is very important and has many applications in various fields (painted canvas and movies restoration, augmented reality, ...). In fact, many images are often scratched or damaged. Let $\Omega \subset \mathbb{R}^d$ $(d = 2, 3)$ denotes the entire image domain. The basic idea is to fill-in an incomplete/damaged region $D \subset \Omega$ based upon the image information available outside D (i.e., in $\Omega \backslash D$) in such a manner, that a viewer can not detect the restored parts. Different techniques have been applied to solve this problem. The early works were based on statistical and algorithmic approaches. Afterward, this kind of problems has drawn a growing attention from the mathematics community. They exploited the well-established theory of Partial Differential Equations (PDE) in image processing problems. Nowadays, PDE models are widely used and are proven to be efficient for solving several image processing problems [7, 8, 11, 19, 20, 23, 29, 34, 35].

The image inpainting, like the image restoration problem, consists in recovering an original image u from an observed one f which is degraded and contaminated with noise. We assume that

$$f = Tu + \eta, \tag{1.1}$$

where η stands for an additive white Gaussian noise and T is a linear degradation

*Mathematics, Information Technology and Applications Laboratory, University of Haute Alsace, France. zakaria.belhachmi@uha.fr

†IPEIT, Université de Tunis, 2, Rue Jawaher Lel Nehru, 1089 Montfleury, Tunisia. mz.kallel@gmail.com

‡National Engineering School at Tunis, University of Tunis-El Manar, B.P. 37, 1002 Tunis-Belvédère, Tunisia. maher.moakher@gmail.com

§LAMSIN-ENIT, University of Tunis-El Manar, B.P. 37, 1002 Tunis-Belvédère, Tunisia. thaljanianis@gmail.com

operator, generally compact (or non invertible). The operator T in the inpainting task is taken to be the indicator function of D. Given f, the problem is then to reconstruct u obeying the model (1.1). The mathematical formulation consists in approximating u by the solution of the following minimization problem:

$$\min_{u\in X} \|Tu - f\|_X^2, \tag{1.2}$$

where X is a Hilbert or a Banach space. One of the major issues of the problem (1.2) is its ill-posedness. In fact, it is unstable with respect to perturbation of the initial data: small changes in the measurements f can result in large changes in the solution u. A classical way to overcome ill-posedness is to add a regularization term [42], i.e., a priori information on u. The regularized problem is formulated as

$$\min_{u\in Y} \left\{G(u) + \|\lambda(u - f)\|_X^2\right\}, \tag{1.3}$$

where $Y \subset X$ and $G : Y \longrightarrow \mathbb{R}$ represents the smoothing effect of the regularization. The Lagrange multiplier λ is such that $\lambda = \lambda_0 >> 1$ in $\Omega\backslash D$ (Full attachment outside inpainting area) and 0 in D (No attachment to the input image f within inpainting area). The first part of (1.3) encodes the image model (smoothing term) and the second is called the fidelity part.

Various types of regularization have been proposed in the literature [11, 20, 23, 34, 35, 38]. The most natural way is to regularize by $G_1(\nabla u)$, where ∇ denotes the gradient operator [20]. This leads to a second-order diffusion equations which are generally unable to connect the edges over large distances (TV model) or they smoothly propagate level lines (harmonic model). They are also unable to reconstruct and keep the curvature because of its higher-order nature. These shortcomings gave rise to a new class of functionals based on high-order derivatives leading to various (higher-order) diffusion models which in general perform better. In fact, such models damp the oscillations and high frequencies (noise) faster than second-order based diffusion models. Moreover, the use of boundary conditions for both the solution $u(x)$ and its derivatives gives a supplementary information on the isoline directions and allows matching edges across large distances.

Overview on higher-order PDE models. Many examples of functionals including higher-order derivatives were proposed. These functionals are focusing on regularization techniques by incorporating second-order derivatives or a sophisticated combination of first- and second-order derivatives. In the pioneering article of A. Chambolle and P.-L. Lions [17], the authors proposed a higher-order method for both image decomposition and restoration. They considered a functional which couples the first- and second-order derivatives by taking into account the Hessian $\nabla^2 u$ in the minimization problem. Since then, similar approaches were widely used in image restoration and inpainting, (see, e.g., [28, 31, 32, 40]), which constitute a straightforward convex combination of first- and second- derivatives in the following general form:

$$\|u - f\|_{L^2(\Omega)} + \int_\Omega G_1(\nabla u)\, dx + \int_\Omega G_2(\nabla^2 u)\, dx, \tag{1.4}$$

where $G_1(\cdot)$ and $G_2(\cdot)$ are given functions.

Recently, the authors in [38] introduced a new non-linear model by the higher-order extension of the well-known Ruden-Osher-Fatemi functional [39] (total variation

minimization). Inspired by the work of Nitzberg et al. in [36], T. Chan et al. proposed in [41] a slightly different model for the Euler-elastica functional. They considered the following functional

$$\|u - f\|_{L^2(\Omega)} + \int_K (a + b\kappa^2)\, d\mathcal{H}^1(x), \tag{1.5}$$

where $\mathcal{H}^1$ is the Hausdorff measure, K is a closed regular subset of Ω and $\kappa = \nabla \cdot (\nabla u/|\nabla u|)$ is the curvature of level sets $\gamma_r : \{x \in K \mid u(x) = r\}$, and a, b are two positive constant weights. It is a higher-order variational method where the regularization term combines the total variation, sensitive to the length of the isolines, and the square of the curvature, which favors curves rather than straight lines. Minimizing the energy (1.5) leads to a highly nonlinear PDE and therefore its numerical solution is a non trivial task and was the subject of many investigations [2, 21, 23, 33].

S. Esedoglu and J. Shen proposed in [23] the Mumford-Shah-Euler image inpainting model. It is a high order correction of the Mumford-Shah model by the minimization of the following energy:

$$F(u, \Gamma) = \frac{\gamma}{2} \int_{\Omega \setminus \Gamma} |\nabla u|^2\, dx + \frac{1}{2} \int_\Omega \lambda(x)(u - f)^2\, dx + \int_\Gamma (a + b\kappa^2)\, d\mathcal{H}^1(x). \tag{1.6}$$

where Γ denotes the set of edges. They gave an efficient numerical realization based on the convergence approximations of Ambrosio and Tortorelli [3, 4], and De Giorgi [26].

Bertozzi, Esedoglu and Gillette proposed in [9, 10] another approach, in the class of fourth-order inpainting algorithms, for binary images using the modified Cahn-Hilliard equation

$$\partial_t u - \Delta(\Delta u - \frac{1}{\epsilon^2} W'(u)) + \lambda(f - u) = 0, \quad \text{in } \Omega. \tag{1.7}$$

where $W(u) = u^2(1 - u)^2$ is a double-well potential and ϵ is a positive parameter that is intended to go to zero. This nonlinear fourth-order PDE, which originated in material sciences [15], describes the evolution of an interface separating two stable states.

A generalization of this Cahn-Hilliard equation, to gray-scale images, was considered in [14]. It is based on H^{-1}-regularization methods which have drawn a growing interest over the last few years. We refer to [11, 30, 37] for more details on this regularization and its impact within image processing problems. The work in [14] consists in a model for inpainting, called $TV - H^{-1}$, where one seeks to minimize an energy that couples the total variation of the image with an H^{-1}-fidelity term. Using the Γ-convergence theory, it was proven that the solution of this $TV - H^{-1}$ model is the L^1-limit of the solution of the Cahn-Hilliard equation when ϵ goes to 0.

The multiscale approach. Most high-order approaches to the restoration or the inpainting problems, make the use of the minimization of an energy of Willmore type, i.e., (1.5). The models obtained this way are generally highly nonlinear and difficult to solve numerically. In another hand, the easiest way to obtain a fourth-order PDE is to minimize $\int_D |\Delta u|^2\, dx$ which leads to the following Euler-Lagrange equation:

$$\Delta^2 u = 0, \text{ in } D, \quad u = f, \text{ on } \partial D \ + \text{ another boundary condition on } \partial D. \tag{1.8}$$

This isotropic fourth-order (stationary) diffusion equation has the benefits of connecting isolines of the image across (large) missing parts while preserving the curvature, however, because of its strong smoothing effect, it cannot capture important features of the image like corners, edges, etc.

In this article, we consider a multiscale approach to construct functionals based on fourth-order PDEs (1.8). More precisely, we consider the following equation:

$$\begin{cases} \Delta(\Delta_\alpha u) + \lambda(u - f) = 0, & \text{in } \Omega, \\ u = f \text{ and } \Delta_\alpha u = 0, & \text{on } \partial\Omega, \end{cases} \tag{1.9}$$

where $\Delta_\alpha u = \nabla(\alpha(x)\nabla u)$. The values of the diffusion function α, which encodes different scales in the image, are dynamically and locally chosen in order to control the amount of smoothing of the operator.

It is known that linear diffusion models are not well-suited for capturing fine geometric structures of an image (edges, corners). However, we prove in this article that our approach allows us to restore such fine features. The reason of this "apparent paradox", is that the adaptive process which is the key of the method, is in fact nonlinear. Loosely speaking, we construct a nonlinear discrete approximation to a continuous linear model, this allows for a dynamical "adaptation of the model" during the processes to make it sensitive to low-order sets and fine features. In addition, the process turns to be convergent, in the Γ-convergence sense, to a Willmore-like functional. Thus, with this approach, we combine at the same framework the simplicity of the linear diffusion models for the image inpainting and, the necessary, nonlinear process for the selection of the diffusion coefficient to capture the singularities.

Organization of the paper. The remainder of this paper is organized as follows: In Section 2, we prove by standard variational techniques the existence and uniqueness of H^1-solution for the image restoration problem. We obtain our equation from a minimization problem −of the regularized functional− based on an H^{-1}-fidelity term. In Section 3, we apply the proposed fourth-order model to image inpainting and we prove the existence of H^1-solutions by means of a fixed point approach. In Section 4, we present the adaptive strategy in details. In particular, we show that it is a two-steps approach where, a mesh-adaptation based on metric error indicator is used to fit the geometry of the computed solution, second, a residual type error indicator is used to locally select the value of α. We perform a Γ-convergence analysis of this process and we show that the solution u generated by the adaptive strategy approximates a solution of a new model which combines the Mumford-Shah functional and the H^{-1}-fidelity term. In Section 5, we consider a new model coupling second and fourth-order derivatives, in analogy with the Euler's elastica model, to improve the overall approach by enforcing both the curvature and the length of the isolines. Finally, we implement our approach in Section 6 and treat several numerical examples to test its efficiency and robustness.

2. Image restoration.

We consider in this section the image restoration problem. In this case, the function λ in (1.9) is taken to be a large constant $\lambda_0 >> 1$ in the image domain Ω.

2.1. Existence and uniqueness of H^1-weak solutions.

We recall that the operator Δ^{-1} is the inverse of the negative operator $-\Delta$ with zero Dirichlet boundary

conditions, i.e., $u = \Delta^{-1} g$ is the unique solution of

$$\begin{cases} -\Delta u = g, & \text{in } \Omega, \\ u = 0, & \text{on } \partial\Omega. \end{cases} \tag{2.1}$$

We define $H^{-1}(\Omega)$ the dual space of $H_0^1(\Omega)$ with corresponding norm $\|\cdot\|_{-1} = \|\nabla \Delta^{-1} \cdot \|_2$ and inner product $\langle \cdot, \cdot \rangle_{-1} = \langle \nabla \Delta^{-1} \cdot, \nabla \Delta^{-1} \cdot \rangle_2$.

The domain Ω is partitioned into N disjoint sub-domains $(\Omega_\ell)_\ell$ such that α is given by the piecewise constant scalar function:

$$\alpha = \alpha_\ell, \text{ in } \Omega_\ell.$$

We denote $\alpha_m = \min\limits_{1 \le \ell \le N} \alpha_\ell > 0$ and $\alpha_M = \max\limits_{1 \le \ell \le N} \alpha_\ell$. We mention that in the restoration case, the function λ is equal to the constant λ_0 in all the domain Ω.

Applying the operator Δ^{-1} to (1.9), we obtain the following problem:

$$\begin{cases} -\Delta_\alpha u + \Delta^{-1}(\lambda_0(u - f)) = 0, & \text{in } \Omega, \\ u = f \text{ and } \Delta_\alpha u = 0, & \text{on } \partial\Omega. \end{cases} \tag{2.2}$$

An H^1-weak solution of the problem (2.2) is defined as a function u in the space $V = \{u \in H^1(\Omega), u|_{\partial\Omega} = f|_{\partial\Omega}\}$, that fulfills

$$\langle \alpha(x) \nabla u, \nabla \phi \rangle_2 - \langle \lambda(f - u), \phi \rangle_{-1} = 0, \ \ \forall \phi \in H_0^1(\Omega). \tag{2.3}$$

Equation (2.3) is a weak formulation of (1.9). In fact, an integration by parts in (2.3) gives:

$$\begin{cases} -\Delta_\alpha u + \Delta^{-1}(\lambda_0(u - f)) = 0, & \text{in } \Omega, \\ \Delta_\alpha \, u = 0, & \text{on } \partial\Omega \end{cases}.$$

By applying the negative Laplace operator $-\Delta$ in the previous system and using the boundary condition $u|_{\partial\Omega} = f|_{\partial\Omega}$, we see that u solves problem (1.9).

Now, to prove the existence of an H^1-weak solution of (1.9), we consider the following minimization problem:

$$\min_{u \in V} J(u), \tag{2.4}$$

where

$$J(u) := \tfrac{1}{2} \int_\Omega \alpha(x) |\nabla u|^2 \, dx + \tfrac{\lambda_0}{2} \|u - f\|_{-1}^2.$$

PROPOSITION 2.1. *Let $f \in L^2(\Omega)$, the functional $J(\cdot)$ admits a unique minimizer $u \in H^1(\Omega)$ with $|u(x)| \le 1$ a.e. in Ω.*

Proof. The functional $J(\cdot)$ is strictly convex. In fact, let u_1 and u_2 be two functions in $H^1(\Omega)$ such that $u_1 \neq u_2$ and $t \in]0, 1[$, we have:

$$\begin{aligned} & tJ(u_1) + (1-t)J(u_2) - J(tu_1 + (1-t)u_2) \\ &= \frac{t(1-t)}{2} \left\{ \int_\Omega \alpha(x) |\nabla u_1|^2 \, dx + \int_\Omega \alpha(x) |\nabla u_2|^2 \, dx - 2 \int_\Omega \alpha(x) \nabla u_1 \cdot \nabla u_2 \, dx \right. \\ &\quad \left. + \lambda_0 \left[\|u_1 - f\|_{-1}^2 + \|u_2 - f\|_{-1}^2 - 2 \int_\Omega \nabla \Delta^{-1}(u_1 - f) \cdot \nabla \Delta^{-1}(u_2 - f) \, dx \right] \right\} \\ &= \frac{t(1-t)}{2} \left\{ \int_\Omega \alpha(x) |\nabla(u_1 - u_2)|^2 \, dx + \lambda_0 \|u_1 - u_2\|_{-1}^2 \right\} > 0. \end{aligned}$$

Furthermore, $J(\cdot)$ is weakly lower semi-continuous in $H^1(\Omega)$. We consider a minimizing sequence $(u_n)_{n\in\mathbb{N}}$ of $J(\cdot)$, i.e.,

$$J(u_n) \underset{n\to\infty}{\longrightarrow} \inf_{u\in V} J(u) = L.$$

Since $\int_\Omega \alpha(x)|\nabla u_n|^2\,dx \le J(u_n)$, $|u_n(x)| \le 1$ for almost every point $x \in \Omega$ and the boundedness of $\alpha(x)$, the sequence $(u_n)_{n\in\mathbb{N}}$ is then uniformly bounded in $H^1(\Omega)$. Therefore, there exists a subsequence, still denoted $(u_n)_{n\in\mathbb{N}}$, such that $u_n \underset{n\to\infty}{\rightharpoonup} u$ weakly in $H^1(\Omega)$ and $u_n \underset{n\to\infty}{\longrightarrow} u$ in $L^p(\Omega)$, for $1 \le p \le \infty$, such that $|u| \le 1$ a.e. in Ω. Thanks to the continuity of the operator $\Delta^{-1} : H^{-1}(\Omega) \longrightarrow L^2(\Omega)$, we get:

$$J(u) \le \liminf_{n\to\infty} J(u_n).$$

The limit u is then a minimizer for $J(\cdot)$. Since V is weakly closed, the minimizer u fulfills the boundary condition $u = f$ on $\partial\Omega$. Uniqueness is guaranteed by the strict convexity of $J(\cdot)$. □

2.2. Remark on the choice of boundary conditions. Contrary to the arbitrariness in the choice of the boundary conditions for the inpainting problem, the Neumann boundary condition is most often used in the restoration of images. In order to have a unified treatment for both problems and for the sake of brevity, we have chosen here to use the Dirichlet conditions.

If we use Neumann conditions, we just have to consider the space

$$V_0 = \left\{ h \in H^1(\Omega);\ \int_\Omega h\,dx = 0 \right\}.$$

Then, in this case we have:

THEOREM 2.2 ([22]). *Let $v \in L^2(\Omega)$, $\int_\Omega v\,dx = 0$. The problem*

$$\begin{cases} -\Delta w = v, & \text{in } \Omega, \\ \frac{\partial w}{\partial n} = 0, & \text{on } \partial\Omega, \end{cases}$$

admits a unique solution in V_0.

Thus, for each $v \in L^2(\Omega)$, $\int_\Omega v\,dx = 0$, we set $w = \Delta^{-1}v$, with w given by Theorem 2.2. The restoration problem may now be expressed as a minimization problem of the energy

$$\min_u \int_\Omega \alpha|\nabla u|^2 + \frac{\lambda_0}{2}\|u - f\|_{-1},$$

and the first order optimality condition gives

$$\begin{cases} -\Delta_\alpha u + \Delta^{-1}(\lambda_0(u - f)) = 0, & \text{in } \Omega, \\ \frac{\partial u}{\partial n} = 0, \quad \frac{\partial(\Delta_\alpha u)}{\partial n} = 0, & \text{on } \partial\Omega. \end{cases} \tag{2.5}$$

Applying the negative Laplacian to this problem, we can also write it as

$$\begin{cases} \Delta(\Delta_\alpha u) + \lambda_0(u - f) = 0, & \text{in } \mathbb{R}_+ \times \Omega, \\ \frac{\partial u}{\partial n} = 0,\ \frac{\partial(\Delta_\alpha u)}{\partial n} = 0, & \text{on } \mathbb{R}_+ \times \partial\Omega. \end{cases}$$

Notice also that, with standard changes, we may consider the "mixed" problem as well

$$\begin{cases} -\Delta_\alpha u + \Delta^{-1}(\lambda_0(u - f)) = 0, & \text{in } \Omega, \\ \frac{\partial u}{\partial n} = 0, \quad \Delta_\alpha u = 0, & \text{on } \partial\Omega. \end{cases} \tag{2.6}$$

2.3. Splitting into two second-order problems. For the sake of simplicity, we assume here that

$$u = 0 \text{ and } \Delta_\alpha u = 0, \text{ on } \partial\Omega. \tag{2.7}$$

The case $u = f$ and $\Delta_\alpha u = 0$, on $\partial\Omega$ can be treated in the same way by choosing a lifting function u^* such that:

$$u^* = f \text{ and } \Delta_\alpha u^* = 0, \text{ on } \partial\Omega,$$

and the proof is not altered by these boundary conditions.

Problem (1.9), viewed as the stationary state of the associated flow, can be splitted into two second-order equations by introducing an auxiliary function w such that:

$$\begin{cases} u_t - \Delta w + \lambda_0(u - f) = 0, & \text{in } \mathbb{R}_+ \times \Omega, \\ -\Delta_\alpha u = w, & \text{in } \mathbb{R}_+ \times \Omega, \\ u = w = 0, & \text{on } \mathbb{R}_+ \times \partial\Omega, \\ u(0, x) = f(x), & \text{in } \Omega. \end{cases} \tag{2.8}$$

The weak formulation reads then: Find a pair $(u, w) \in H_0^1(\Omega) \times H_0^1(\Omega)$, $u(0, x) = f(x)$, such that:

$$\begin{cases} \langle \partial_t u, \phi\rangle_2 + \langle \nabla w, \nabla\phi\rangle_2 + \langle \lambda_0 u, \phi\rangle_2 = \langle \lambda_0 f, \phi\rangle_2, & \forall \phi \in H_0^1(\Omega), \\ \langle \alpha\nabla u, \nabla\psi\rangle_2 - \langle w, \psi\rangle_2 = 0, & \forall \psi \in H_0^1(\Omega). \end{cases} \tag{2.9}$$

It is easy to verify that the pair $(u, w = \Delta_\alpha u)$ is a weak solution of (2.9) where u is the solution for problem (1.9). To prove uniqueness, let the pair $(u_1, w_1) \in H_0^1(\Omega) \times H_0^1(\Omega)$ be another solution of the system (2.9), we then have:

$$\begin{cases} \langle \partial_t(u - u_1), \phi\rangle_2 + \langle \nabla(w - w_1), \nabla\phi\rangle_2 + \langle \lambda_0(u - u_1), \phi\rangle_2 = 0, & \forall \phi \in H_0^1(\Omega), \\ \langle \alpha\nabla(u - u_1), \nabla\psi\rangle_2 - \langle (w - w_1), \psi\rangle_2 = 0, & \forall \psi \in H_0^1(\Omega). \end{cases}$$

Picking $\psi = (w - w_1)$ in the second equation, we have the identity

$$\langle w - w_1, w - w_1\rangle_2 = \langle \alpha\nabla(u - u_1), \nabla(w - w_1))\rangle_2. \tag{2.10}$$

By choosing the test function $\phi = u - u_1$ in the first equation and using (2.10) and the positivity of α, we obtain:

$$\langle \partial_t(u - u_1), u - u_1\rangle_2 = -\langle \nabla(u - u_1), \nabla(w - w_1))\rangle_2 - \langle \lambda_0(u - u_1), (u - u_1)\rangle_2 \leq 0.$$

So that

$$\partial_t(\|u(t) - u_1(t)\|_2^2) = 2\langle \partial_t(u - u_1), u - u_1\rangle_2 \geq 0.$$

It follows that the function $t \mapsto \|u(t) - u_1(t)\|_2^2$ is decreasing on $\mathbb{R}_+$. Since $u(0) = u_1(0)$, we get $u = u_1$ which implies that $w = w_1$.

3. Image inpainting problem. We study in this section the image inpainting problem by considering the following system:

$$\begin{cases} \partial_t u + \Delta(\Delta_\alpha u) + \lambda(x)(u-f) = 0, & \text{in } \mathbb{R}_+ \times \Omega, \\ u = f \text{ and } \Delta_\alpha u = 0, & \text{on } \mathbb{R}_+ \times \partial\Omega, \\ u(0,x) = f, & \text{in } \Omega. \end{cases} \tag{3.1}$$

The only difference here is the Lagrange multiplier λ which takes the value 0 in D and $\lambda_0 >> 0$ in $\Omega \backslash D$. Solving the minimization problem (2.4) by means of Euler-Lagrange equation for such choice of λ does not give the fourth-order PDE (3.1). In fact, this minimization problem exhibits the following optimality condition:

$$-\Delta_\alpha u + \lambda(x)\Delta^{-1}(\lambda(x)(u-f)) = 0. \tag{3.2}$$

3.1. Existence of H^1-weak solution of the stationary equation. Following the methodology used in [14] to prove the existence of H^1-weak solution by means of Schauder's fixed-point theorem

PROPOSITION 3.1 (Schauder's fixed-point theorem [24]). *Assume that $K \subset X$ is a compact and convex set and that $A : K \longrightarrow K$ is continuous. Then A admits a fixed point.*

Consider the following intermediate minimization problem:

$$\min_{u \in V} F(u,v), \tag{3.3}$$

where

$$F(u,v) = H(u) + \tfrac{1}{2}\|\lambda_0 u - \lambda f - (\lambda_0 - \lambda)v\|_{-1}^2, \tag{3.4}$$

where f and $v \in L^2(\Omega)$ and $H(u) = \int_\Omega \frac{\alpha(x)}{2}|\nabla u|^2\, dx$. The Euler-Lagrange equation corresponding to (3.3) writes:

$$\begin{cases} -\Delta_\alpha u - \Delta^{-1}(\lambda(f-u) + (\lambda_0 - \lambda)(v-u)) = 0, & \text{in } \Omega, \\ u = f \text{ and } \Delta^{-1}(\lambda(f-u) + (\lambda_0 - \lambda)(v-u)) = 0, & \text{on } \partial\Omega. \end{cases} \tag{3.5}$$

Its weak formulation is: Find $u \in H_0^1(\Omega)$ such that:

$$\langle \alpha \nabla u, \nabla \phi \rangle_2 - \langle (\lambda(f-u) + (\lambda_0 - \lambda)(v-u)), \phi \rangle_{-1} = 0, \ \ \forall \phi \in H_0^1(\Omega). \tag{3.6}$$

PROPOSITION 3.2. *Let f and $v \in L^2(\Omega)$, the functional $F(\cdot, v)$ admits a unique minimizer $u \in H^1(\Omega)$ with $|u(x)| \leq 1$ a.e. in Ω.*

Proof. For a fixed $v \in L^2(\Omega)$, the existence and uniqueness of the minimizer u can be obtained by the same technique used in the restoration case in Proposition 2.1. □

Let $A : L^2(\Omega) \longrightarrow L^2(\Omega)$ be the operator such that $A(v) = u$ is the unique solution of (3.6). Therefore, a fixed point of the operator A, i.e., a solution $u = v$, is then a solution of the equation (3.1).

PROPOSITION 3.3. *Let $f \in L^2(\Omega)$, the operator A admits a fixed point $u \in H^1(\Omega)$ with $|u(x)| \leq 1$ a.e. in Ω. Moreover, u is H^1-weak solution of the stationary equation of (3.1).*

Proof. Let $R = |\Omega|^{1/2}$ and a function $v \in B(0,R)$ (where $B(0,R)$ denotes the ball in $L^2(\Omega)$ with center 0 and radius R). From Proposition 3.2, the minimization

problem (3.4) admits a unique minimizer $u = A(v)$ in the space $H^1(\Omega)$ such that $|u(x)| \leq 1$ a.e. in Ω. Then, it is an element of $B(0,R)$. Furthermore, it is well known that the mapping $H^1(\Omega) \hookrightarrow L^2(\Omega)$ is a compact embedding. The operator A then maps $L^2(\Omega) \to K$, where K is a compact subset of $L^2(\Omega)$. Thus we have:

$$A : B(0,R) \longrightarrow B(0,R) \cap K = \tilde{K},$$

where $\tilde{K}$ is a compact and convex subset of $L^2(\Omega)$. To apply Schauder's fixed-point theorem, it remains to prove that A is continuous in $B(0,R)$. Let $(v_k)_{k\geq 0}$ be a sequence which converges to $v \in L^2(\Omega)$ and $A(v_k) = u_k$. The function u_k is then the unique minimizer of (3.4) associated with v_k, and we have: $F(u_k, v_k) \leq F(0, v_k)$, i.e.,

$$F(u_k, v_k) \leq \tfrac{1}{2}\|\lambda f + (\lambda_0 - \lambda)v_k\|_{-1}^2.$$

Since $L^2(\Omega) \hookrightarrow H^{-1}(\Omega)$, we get $\|v_k\|_{-1} \leq C\|v_k\|_{L^2(\Omega)} \leq CR$ and also $\|\lambda v_k\|_{-1} \leq C'$ for some given constants $C, C' > 0$. Accordingly, we obtain the following estimate:

$$F(u_k, v_k) \leq C\lambda_0(|\Omega| + |D|), \quad C > 0.$$

and then $(u_k)_{k\geq 0}$ is uniformly bounded in $H^1(\Omega)$. Thus, we can consider a convergent subsequence $u_{k_j} \underset{j\to\infty}{\rightharpoonup} u \in H^1(\Omega)$ and $u_{k_j} \underset{j\to\infty}{\longrightarrow} u$ in $L^2(\Omega)$. Hence, the unique (weak) solution $A(v_k) = u_k$ of (3.6) weakly converges to the unique weak solution u of

$$\Delta_\alpha u + \Delta^{-1}(\lambda(f-u) + (\lambda_0 - \lambda)(v-u)) = 0.$$

From the uniqueness of the minimizers of (3.4), we obtain $u = A(v)$. We then deduce that A is continuous in $L^2(\Omega)$ and the existence of a stationary solution u follows from Schauder's fixed-point theorem. In addition, this solution verifies:

$$\begin{cases} \Delta_\alpha u + \Delta^{-1}(\lambda(f-u)) = 0, & \text{in } \Omega, \\ u = f \text{ and } \Delta_\alpha\, u = 0, & \text{on } \partial\Omega, \end{cases}$$

or equivalently, the system (1.9). □

3.2. Decoupling into two Poisson equations. Like for the restoration case, we shall use the boundary conditions

$$u = 0 \text{ and } \Delta_\alpha u = 0, \text{ on } \partial\Omega.$$

We split the fourth-order equation (3.1) into two Poisson equations by introducing the auxiliary function w such that:

$$\begin{cases} \partial_t u - \Delta w + \lambda(u-f) = 0, & \text{in } \mathbb{R}_+ \times \Omega, \\ -\Delta_\alpha u = w, & \text{in } \mathbb{R}_+ \times \Omega, \\ u = w = 0, & \text{on } \mathbb{R}_+ \times \partial\Omega. \end{cases}$$

The weak formulation reads: Find the pair $(u,w) \in H_0^1(\Omega) \times H_0^1(\Omega)$, $u(0) = f$, such that:

$$\begin{cases} \langle \partial_t u, \phi\rangle_2 + \langle \nabla w, \nabla\phi\rangle_2 + \langle \lambda u, \phi\rangle = \langle \lambda f, v\rangle_2, & \forall \phi \in H_0^1(\Omega), \\ \langle \alpha\nabla u, \nabla\psi\rangle_2 - \langle w, \psi\rangle_2 = 0, & \forall \psi \in H_0^1(\Omega). \end{cases} \tag{3.7}$$

3.3. Time-discretization. We use the semi-implicit Euler scheme. We denote by $\frac{u-u^{old}}{dt}$ an approximation of $\partial_t u$, where u^{old} and u are the solutions at time t_{old} and $t = t_{old} + dt$, respectively. We obtain the following semi discrete problem:

$$\begin{cases} \langle \frac{u-u^{old}}{dt}, \phi\rangle_2 + \langle \nabla w, \nabla\phi\rangle_2 + \langle \lambda u, \phi\rangle = \langle \lambda f, v\rangle_2, & \forall \phi \in H_0^1(\Omega), \\ \langle \alpha\nabla u, \nabla\psi\rangle_2 - \langle w, \psi\rangle_2 = 0, & \forall \psi \in H_0^1(\Omega). \end{cases} \tag{3.8}$$

PROPOSITION 3.4. *For a fixed $u^{old} \in H_0^1(\Omega)$, the problem (3.8) admits a solution $(u, w) \in H_0^1(\Omega) \times H_0^1(\Omega)$.*

Proof. For a given $v \in L^2(\Omega)$, $u^{old} \in H_0^1(\Omega)$ and $dt > 0$, we define the following energy

$$F(u, v) + \frac{1}{2}\|\frac{u-u^{old}}{dt}\|_{-1}^2. \tag{3.9}$$

Thus, the same arguments as in the proof of Theorem 3.3 yield the existence and uniqueness of the minimizer $u \in H^1(\Omega)$ and we prove, thanks to the properties of the operator $A : L^2(\Omega) \longrightarrow L^2(\Omega)$, that the fixed point u is given by:

$$\begin{cases} \frac{u-u^{old}}{dt} + \Delta(\Delta_\alpha u) + \lambda(f-u) = 0, & \text{in } \Omega, \\ u = 0 \text{ and } \Delta_\alpha u = 0, & \text{on } \partial\Omega. \end{cases}$$

The pair $(u, w = \Delta_\alpha u)$ then satisfies the system (3.8). □

4. Discrete problem and adaptive strategy. We assume that the domain Ω is polygonal. We consider a regular family of triangulations $\mathbb{T}_h$ made of element which are triangles (or quadrilaterals) with a maximum size h, satisfying the usual admissibility assumptions, i.e., the intersection of two different elements is either empty, a vertex, or a whole edge. For $h > 0$, we introduce the following discrete space:

$$X_h = \left\{ v_h \in C(\overline{\Omega}) | \forall K \in \mathbb{T}_h, v_h|_K \in P_1(K) \right\} \cap H_0^1(\Omega).$$

In the same way as the continuous case, we can easily prove that in both the inpainting and the restoration cases, the discrete version admits a solution $(u_h, w_h) \in X_h \times X_h$. This unique solution solves the same system (3.8) where the space $H_0^1(\Omega)$ is replaced by X_h.

4.1. Adaptive procedure. For each element $K \in \mathbb{T}_h$, the following local discrete energy

$$\eta_K = \alpha_K^{\frac{1}{2}} \|\nabla u_{\alpha,h}\|_{L^2(K)}, \tag{4.1}$$

contains some information on the error distribution of the computed solution $u_{\alpha,h}$. In fact, the discontinuities (edges) are contained in regions where the brightness changes sharply and consequently where this error indicator is large. Moreover, it may be proved that the gradient of $u_{\alpha,h}$ captures this change in brightness and its magnitude provides an information about the "strength" of the edges (see [6]). Thus, the quantity (4.1) acts as an edge detector and locates such regions. This particularity makes it well suited to control and locally select the diffusion coefficient α using the following algorithm:

Algorithm 1

1. Start with the initial grid $\mathbb{T}_h^0$ corresponding to the image.
2. **Adaptive steps:**
   - Compute $u_{\alpha_0,h}$ on $\mathbb{T}_h^0$ with a large constant $\alpha = \alpha^0$.
   - Build an adapted mesh $\mathbb{T}_h^1$ (in the sense of the finite element method, i.e., with respect to the parameter h) with a metric error indicator.
   - In the locations where η_K is large (with respect to its mean value), we perform a local choice of $\alpha(x)$ on $\mathbb{T}_h^1$ to obtain a new function $\alpha_1(x)$.
3. Go to steps 1. and 2. and compute $u_{\alpha_1,h}$ on $\mathbb{T}_h^1$.

During the adaptation, we use the following formula for each triangle K;

$$\alpha_K^{k+1} = \max\left(\frac{\alpha_K^k}{1+\kappa * \left(\left(\frac{\eta_K}{\|\eta\|_\infty}\right) - 0.1\right)^+}, \alpha_{trh}\right),$$

where α_{trh} is a threshold parameter and κ is a coefficient chosen to control the rate of decrease in α, $(u^+) = \max(u, 0)$.

REMARK 4.1. *There are other possible choices for this formula as it will appears in the* Γ*-convergence analysis. The one given here is that implemented for the numerical computations. Loosely speaking, it may be viewed as follows: in the regions of high gradients, it decreases the values of* α *when the error indicator deviates more then 10% from its mean value.* α *decreases nearly as a geometric sequence with the iteration number, until a given threshold is attained.*

Let us give more details on the implementation of this algorithm. First, we build an adapted mesh $\mathbb{T}_h^1$ (in the sense of finite-element method, i.e., with respect to the parameter h). The description of the adapted triangulation is the following: close to the jump sets of $u_{\alpha,h}$, the error is large, we then cut the element K into a finite number of smaller elements to decrease such an error and to fit the edges, while, far from these jump sets, there is no restriction on how to choose the triangles and the initial grid is coarsened. This produce meshes with small number of degrees of freedom in the homogeneous area. Second, we make an "optimal" choice of the function α, following the map furnished by the error indicator $(\eta_K)_{K\in\mathbb{T}_h}$, on each element K. Thus, we may decrease the value of α in order to correctly approximate the edges.

REMARK 4.2. *It is easily seen that if* u *wants to jump across a triangle* K *then* η_K *tends to* $+\infty$ *and thus* α_K *is chosen such that it tends to* 0*, otherwise* η_K *tends to 0 and* α_K *remains constant. The overall decrease of the global error is guaranteed by a balance between the energy in these two parts of the domain. Chosen this way, the function* α *plays in the present context a role similar to that of the* z*-field in the Ambrosio-Tortorelli approximation for the Mumford-Shah energy.*

4.2. Γ-convergence analysis for the adaptive algorithm. In this section, we motivate our approach by analyzing the limit behavior of the solution generated by the adaptive algorithm. More precisely, we want to prove that this approach allows to approximate, in the Γ-convergence sense, a new model that couples a Mumford-Shah function with an H^{-1}-term, which we will call MS$-H^{-1}$. Before starting our discussion, let us recall the definition of the Γ-convergence and its impact within the

study of optimization problems. For more details on Γ-convergence we refer the reader to [12].

DEFINITION 4.3. *Let $X = (X, d)$ be a metric space and $(G_\epsilon)_{\epsilon>0}$ be family of functions $G_\epsilon : X \longrightarrow [0, +\infty)$. We say that the function (G_ϵ) Γ-converges to the function $G : X \longrightarrow [0, +\infty)$ on X as $\epsilon \longrightarrow 0$ if $\forall x \in X$ we have:*

i) For every sequence $(x_\epsilon)_\epsilon$ such that $d(x_\epsilon, x) \longrightarrow 0$ we have

$$G_\epsilon(x) \leq \liminf G_\epsilon(x_\epsilon)$$

ii) There exists a sequence $(x_\epsilon)_\epsilon$ such that $d(\overline{x}_\epsilon, x) \longrightarrow 0$ and

$$G_\epsilon(x) = \lim G_\epsilon(\overline{x}_\epsilon).$$

Then, G is the Γ-limit of G_ϵ in X and we write: $G(x) = \Gamma - \lim_\epsilon G_\epsilon(x)$, $x \in X$.

PROPOSITION 4.4. *Assume $(G_\epsilon)_\epsilon$ Γ-converges to G, and for every $\epsilon > 0$, let u_ϵ be a minimizer of G_ϵ over X. Then, if a (sub)sequence of $(x_\epsilon)_\epsilon$ converges to $x \in X$, we have u is a minimizer of G and $(G(x_\epsilon))_\epsilon$ converges to $G(x)$.*

REMARK 4.5. *If $F : X \longrightarrow [-\infty, +\infty]$ is continuous and $(G_\epsilon)_\epsilon$ Γ-converges to G then $(F + G_\epsilon)_\epsilon$ Γ-converges to $F + G$.*

Γ-convergence analysis. A Γ-convergence study of this adaptive strategy was presented in [5] for optic flow estimation. The authors proved that this algorithm is equivalent to the adaptive one introduced by Chambolle-Dal Maso [18] and Chambolle-Bourdin [16]. The last authors introduced an implementation of a approximation of Mumford-Shah functional that makes an extensive use of the mesh adaptation techniques. The numerical implementation and the mathematical properties of this method were proposed and detailed in [18].

We briefly recall the results and the numerical approximation of this method. For a fixed angle $0 < \theta_0 \leq 2\pi/3$, a constant $c \geq 6$, and for $\epsilon > 0$, we set $\mathcal{T}_\epsilon(\Omega) = \mathcal{T}_\epsilon(\Omega; \theta_0; c)$ be the set of all triangulations of Ω whose triangles K have the following characteristics:

i) The length of all three edges of K is between ϵ and ϵc.
ii) The three angles of K are greater than or equal to θ_0.

Let $V_\epsilon(\Omega)$ the set of all continuous functions $u : \Omega \longrightarrow \mathbb{R}$ such that u is affine on any triangle K of a triangulation $\mathbb{T} \in \mathcal{T}_\epsilon(\Omega)$ and for a given u, $\mathcal{T}_\epsilon(u) \subset \mathcal{T}_\epsilon(\Omega)$ is the set of all triangulations adapted to the function u, i.e., such that u is piecewise affine on $\mathbb{T}$. They introduce a non-decreasing continuous function $g : [0, +\infty) \longrightarrow [0, +\infty)$ such that:

$$\lim_{t\to 0} \frac{g(t)}{t} = 1, \ \lim_{t\to+\infty} g(t) = g_\infty.$$

For any $u \in L^p(\Omega), (p \geq 1)$ and $\mathbb{T} \in \mathcal{T}_\epsilon(\Omega)$, the authors in [18] introduced the following minimization problem:

$$G_\epsilon(u) = \min_{\mathbb{T}\in\mathcal{T}_\epsilon(\Omega)} \tilde{G}_\epsilon(u, \mathbb{T}), \tag{4.2}$$

where

$$\tilde{G}_\epsilon(u, \mathbb{T}) = \begin{cases} \sum_{K\in\mathbb{T}} |K \cap \Omega| \dfrac{1}{h_K} g(h_K |\nabla u|^2), & u \in V_\epsilon(\Omega), \mathbb{T} \in \mathcal{T}_\epsilon(\Omega), \\ +\infty, & \text{Otherwise.} \end{cases}$$

For ϵ going to zero and provided θ_0 is less than some $\Theta > 0$, they proved that the energy G_ϵ Γ-converges to the Mumford-Shah functional:

$$G(u) = \begin{cases} \int_\Omega |\nabla u(x)|^2\,dx + g_\infty \mathcal{H}^1(S_u), & u \in L^2(\Omega) \cap GSBV(\Omega) \\ +\infty, & u \in L^2(\Omega) \backslash GSBV(\Omega). \end{cases}$$

where is $GSBV(\Omega)$ the generalized special function of bounded variation (see [1]).

It follows from the result of the Γ-convergence of G_ϵ to G, see [18, Theorem 2], the continuity of the second term of the functional in $L^2(\Omega)$ (follows from the continuity of Δ^{-1}, i.e., the stability in the elliptic problems) and the Remark 4.2.

PROPOSITION 4.6. *Let f and v in $L^2(\Omega)$ be two given functions and $\epsilon > 0$ be a positive parameter. Therefore we have:*

i) The sequence of functionals

$$G_\epsilon(u) + \frac{\lambda_0}{2}\|u - f\|_{-1}^2,$$

Γ-converges for $\epsilon \longrightarrow 0$ in the topology of $L^2(\Omega)$ to

$$G(u) + \frac{\lambda_0}{2}\|u - f\|_{-1}^2,$$

and u_{ϵ_j} converges strongly to u in the topology of $L^2(\Omega)$.

ii) The sequence of functionals

$$G_\epsilon(u) + \tfrac{1}{2}\|\lambda_0 u - \lambda f - (\lambda_0 - \lambda)v\|_{-1}^2,$$

Γ-converges for $\epsilon \longrightarrow 0$ in the topology of $L^2(\Omega)$ to

$$G(u) + \tfrac{1}{2}\|\lambda_0 u - \lambda f - (\lambda_0 - \lambda)v\|_{-1}^2.$$

Let ψ be the Legendre-Fenchel transform of g. For a given triangulation $\mathbb{T}_\epsilon$, it was proven in [18] that the minimization of G_ϵ is equivalent to the minimization of the following functional:

$$G'_\epsilon(u, v, \mathbb{T}_\epsilon) = \sum_{K \in \mathbb{T}_\epsilon} |K \cap \Omega| \frac{1}{h_K}(v_K |\nabla u|^2 + \frac{\psi(v_K)}{h_K}),$$

over all $u \in V_\epsilon(\Omega)$ and $v = (v_K)_{K \in \mathcal{T}_\epsilon}$, piecewise constant on each $K \in \mathcal{T}_\epsilon$. For a fixed u, the minimizer over each v is explicitly given by:

$$v_K = g'(h_K |\nabla u|^2). \tag{4.3}$$

The iterative method used in [18] is then similar to the adaptive strategy presented in this paper and the local choice of α using the error indicator η_K^2 is similar of the choice of v_K in (4.3) with $v = \alpha$.

REMARK 4.7. *The analysis presented here is carried out with the Neumann boundary conditions on u (e.g. problem (2.6) or (2.5)), which is the framework used in [5, 16, 18] for a denoising problem or optic flow estimation. The application to the Dirichlet case requires some (tedious but non-essential) modifications and the result still holds.*

REMARK 4.8. *Note that, like for second-order models, different PDE-based approaches might yield a Γ-limit approximation of the Mumford-Shah model. Given a function α, the computation of the solution u is simple and fast. In fact, after each adaptation step the number of nodes of the adapted mesh can be reduced.*

5. Coupled fourth- and second-order derivatives. In this section, we give a sophisticated combination of first and second-order derivatives and we apply the adaptive strategy without giving a Γ-convergence analysis. We prove the existence of stationary solution of the following equation:

$$\begin{cases} \partial_t u + a\Delta_\beta(\Delta_\alpha u) - b\Delta_\beta u + \lambda(u-f) = 0, & \text{in } \mathbb{R}_+ \times \Omega, \\ u = f \text{ and } \Delta_\alpha u = 0, & \text{on } \mathbb{R}_+ \times \partial\Omega, \\ u(0,x) = f, & \text{in } \Omega. \end{cases} \tag{5.1}$$

where $a, b > 0$ are two weighting constant parameters. We have set β as diffusion coefficient in the second-order term in the system (5.1). This choice allows us to provide the existence of a H^1-weak solution for (5.1) when dealing with boundary condition $u = f$ and $\Delta_\alpha u = 0$, on $\partial\Omega$.

This model might be considered as a simplified version of the Euler's elastica model, where the curvature and the length terms are replaced by the fourth- and second-order derivatives, respectively. The parameters a and b are used to control the trade off between the length and curvature in analogy with Euler's elastica model. Various works were interested with the elastica equation and its numerical solution. Esedoglu and Shen [23] proposed the Mumford-Shah-Euler inpainting model, based on the Γ-convergence approximations of Ambrosio & Tortorelli [3, 4] and De Giorgi [25]. We emphasize that in our approach, the computation of numerical solutions is relatively simple contrary to the elastica model where the numerics is difficult and the algorithms are very slow (see [13, 21]).

Let the operator Δ_β^{-1} be the inverse of the negative operator $-\Delta_\beta$ with zero Dirichlet boundary conditions, i.e., $u = \Delta_\beta^{-1} g$ is the unique solution of

$$\begin{cases} -\Delta_\beta u = g, & \text{in } \Omega, \\ u = 0, & \text{on } \partial\Omega. \end{cases} \tag{5.2}$$

We set $\langle \cdot, \cdot \rangle_{-1,\beta} = \langle \beta^{\frac{1}{2}} \nabla \Delta_\beta^{-1} \cdot, \beta^{\frac{1}{2}} \nabla \Delta_\beta^{-1} \cdot \rangle_2$ the inner product in $H^{-1}(\Omega)$ the dual space of $H_0^1(\Omega)$ with corresponding norm $\| \cdot \|_{-1,\beta} = \| \beta^{\frac{1}{2}} \nabla \Delta_\beta^{-1} \cdot \|_2$.

5.1. Existence of H^1-weak solution of the stationary equation. We shall prove the existence of a H^1-weak solution for the model (5.1) using the same techniques for the equation (3.1).

The theoretical study in this case is valid only for the boundary conditions

$$u = \Delta_\alpha u = 0, \quad \text{on } \partial\Omega.$$

If not, we take a lifting function u^* which verifies (2.7) and the proof remains valid for $w = u - u^*$. By applying the operator Δ_β^{-1}, the system (5.1) can be equivalently rewritten as:

$$\begin{cases} -a\Delta_\alpha u + bu + \Delta_\beta^{-1}(\lambda(u-f)) = 0, & \text{in } \Omega, \\ u = 0 \text{ and } \Delta_\alpha\, u = 0, & \text{on } \partial\Omega. \end{cases} \tag{5.3}$$

For a given $\tau > 0$ and $v \in L^2(\Omega)$, we define the following energy

$$J_\beta(u,v) = aG(u) + \frac{b}{2}\|u\|_2^2 + \frac{1}{2}\|\lambda_0 u - \lambda f - (\lambda_0 - \lambda)v\|_{-1,\beta}^2. \tag{5.4}$$

The functional $J_\beta(\cdot, v)$ admits a unique minimizer $u \in H^1(\Omega)$ with $|u(x)| \leq 1$ a.e. in Ω and which verifies the following weak formulation:

$$b\langle u, \phi\rangle_2 + a\langle \alpha\nabla u, \nabla\phi\rangle_2 - \langle(\lambda(f-u) + (\lambda_0 - \lambda)(v-u)), \phi\rangle_{-1,\beta} = 0. \tag{5.5}$$

Let $A : L^2(\Omega) \longrightarrow L^2(\Omega)$ such that for a given $v \in L^2(\Omega)$, we associate $A(v) = u$ the unique solution of the weak problem (5.5). Therefore, it is easy to verify that a fixed point of A is a solution for (5.1). Following the same lines of the analysis carried out for the previous model we have:

PROPOSITION 5.1. *The operator A admits a fixed point $u \in H^1(\Omega)$ with $|u(x)| \leq 1$ a.e. in Ω. Moreover, u is H^1-weak stationary solution of the equation (5.1).*

PROPOSITION 5.2. *Let f and v in $L^2(\Omega)$ be two given functions and $\epsilon > 0$ be a positive parameter. We have:*

i) The sequence of functionals

$$a\, G_\epsilon(u_\epsilon) + \frac{b}{2}\|u_\epsilon\|_2^2 + \frac{\lambda_0}{2}\|u_\epsilon - f\|_{-1}^2,$$

Γ-converges for $\epsilon \longrightarrow 0$ in the topology of $L^2(\Omega)$ to

$$a\, G(u) + \frac{b}{2}\|u\|_2^2 + \frac{\lambda_0}{2}\|u - f\|_{-1}^2,$$

and u_ϵ converges strongly to u in the topology of $L^2(\Omega)$.

ii) The sequence of functionals

$$a\, G_\epsilon(u_\epsilon) + \frac{b}{2}\|u_\epsilon\|_2^2 + \tfrac{1}{2}\|\lambda_0 u_\epsilon - \lambda f - (\lambda_0 - \lambda)v\|_{-1}^2,$$

Γ-converges for $\epsilon \longrightarrow 0$ in the topology of $L^2(\Omega)$ to

$$a\, G(u) + \frac{b}{2}\|u\|_2^2 + \frac{b}{2}\|u_\epsilon\|_2^2 + \frac{1}{2}\|\lambda_0 u_\epsilon - \lambda f - (\lambda_0 - \lambda)v\|_{-1}^2.$$

5.2. Splitting into two Poisson equations. We assume here that

$$u = 0 \text{ and } \Delta_\alpha u = 0, \text{ on } \partial\Omega,$$

and we split the fourth-order equation (5.1) into two second-order equations as follows:

$$\begin{cases} \partial_t u - a\Delta_\beta w - b\Delta_\beta u + \lambda(u - f) = 0, & \text{in } \mathbb{R}_+ \times \Omega, \\ -\Delta_\alpha u = w, & \text{in } \mathbb{R}_+ \times \Omega, \\ u = w = 0, & \text{on } \mathbb{R}_+ \times \partial\Omega, \\ u_0 = f, & \text{in } \Omega. \end{cases}$$

The weak formulation is to find a pair $(u, w) \in H_0^1(\Omega) \times H_0^1(\Omega)$, $u(0) = f$, such that:

$$\begin{cases} \langle \partial_t u, \phi\rangle_2 + b\langle \beta\nabla u, \nabla\phi\rangle_2 + a\langle \beta\nabla w, \nabla\phi\rangle_2 + \langle \lambda u, \phi\rangle_2 = \langle \lambda f, v\rangle_2, & \forall \phi \in H_0^1(\Omega), \\ \langle \alpha\nabla u, \nabla\psi\rangle_2 - \langle w, \psi\rangle_2 = 0, & \forall \psi \in H_0^1(\Omega). \end{cases} \tag{5.6}$$

5.3. Time-discretization. We consider the following semi-implicit Euler scheme:

(5.7)
$$\begin{cases} \langle \dfrac{u-u^{old}}{dt}, \phi\rangle_2 + b\langle \beta\nabla u, \nabla\phi\rangle_2 + a\langle \beta\nabla w, \nabla\phi\rangle_2 + \langle \lambda u, \phi\rangle_2 = \langle \lambda f, v\rangle_2, & \forall \phi \in H_0^1(\Omega), \\ \langle \alpha\nabla u, \nabla\psi\rangle_2 - \langle w, \psi\rangle_2 = 0, & \forall \psi \in H_0^1(\Omega). \end{cases}$$

PROPOSITION 5.3. *For a fixed $u^{old} \in H_0^1(\Omega)$, the problem (3.7) admits a solution $(u, w) \in H_0^1(\Omega) \times H_0^1(\Omega)$.*

Proof. For a given $v \in L^2(\Omega)$, $u^{old} \in H_0^1(\Omega)$ and $dt > 0$, we define the following energy

$$J_\beta(u, v) + \| \frac{u-u^{old}}{dt} \|^2_{-1,\beta}. \tag{5.8}$$

By the same techniques as in Theorem 2.2, we can prove the existence and uniqueness of a minimizer $u \in H^1(\Omega)$ and we can prove that the operator, $A : L^2(\Omega) \longrightarrow L^2(\Omega)$ such that for a given $v \in L^2(\Omega)$, we associate $A(v) = u$ the unique minimizer of (5.8), admits a fixed point u which verifies:

$$\begin{cases} \frac{u-u^{old}}{dt} + a\Delta_\beta(\Delta_\alpha u) - b\Delta_\beta u + \lambda(u-f) = 0, & \text{in } \Omega, \\ u = 0 \text{ and } \Delta_\alpha u = 0, & \text{on } \partial\Omega \end{cases} \tag{5.9}$$

By operator splitting, it is easy to verify that $(u, w = \Delta_\alpha u)$ is a weak solution to (5.7). □

6. Numerical examples. In this work, all the PDEs are solved with the open source software FreeFem++ [27]. In all examples, the damaged/missed regions are delimited by the red contour.

6.1. Image restoration. We begin by testing our approach for an image denoising problem. In the left-hand plot of Fig. 1, we display the original (binary) image with a squared domain (120×120 pixels). In the middle, we display the noisy image f, obtained by adding a Gaussian noise, whereas the right-hand plot shows the restored one obtained by using our approach (1.9).

We initialized the algorithm with a large value of $\alpha = 50$ and we performed 20 iterations of the adaptive algorithm. We plot in Fig. 2 the mesh, the function α and the error indicator at convergence. The latter indicates the regions where we have edges whereas α_K plays in the present context a role similar to that of the z-field in the Ambrosio-Tortorelli approximation method for the Mumford-Shah energy. We can also see the "sparsification" effect on the mesh in the left-hand plot of Fig. 2, which emphasizes the low cost of the method.

We tested our model on gray-scale image (200×200 pixels) in Fig. 3 where we displayed the original (noisy) image and the restored one.

6.2. Image inpainting. We give some examples for the application of our proposed approach to image inpainting. The goal is to reconstruct the missing information in the red parts, i.e.,D, by the diffusion of the information from the intact part, i.e, $\Omega\backslash D$.

6.2.1. Curvature inpainting. We give in the following the numerical results for the two adaptive inpainting approaches (3.1) and (5.1). For the model (5.1), we took $\alpha = \beta$ and both of them were updated simultaneously (with the same formula

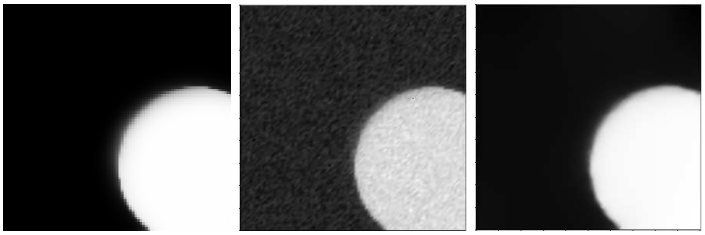

FIG. 1. *Original, noisy and restored images, respectively.*

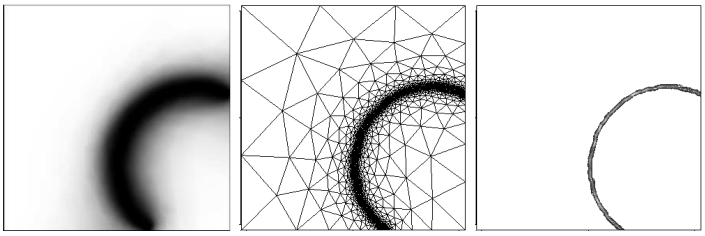

FIG. 2. *The function α, the mesh and η at convergence.*

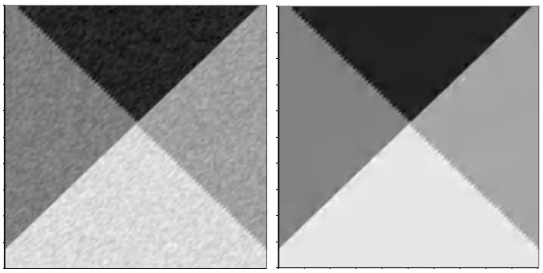

FIG. 3. *The noisy and the restored images.*

of Algorithm 1). In Fig. 5, we present the reconstruction of quarter of a circle using the model (3.1). We display the evolution of the restored image for iterations 1, 5 and 20. In the first iteration (α is constant), we solved a biharmonic equation which gives a curved, but a very smooth (blurred), edge in D. We can see the efficiency of the adaptation process in the damaged region where the edge was inpainted sharply by simultaneously keeping its curvature.

In Fig. 6, we tested the adaptive algorithm for different values of the ratio $\frac{b}{a}$ in equation (5.1), in order to show the effects of each term (the fourth- and second-order one). We plot in Fig. 6 the restored images at the end of algorithm. It appears that if more weight is set on the second-order derivatives in (5.1), then the inpainted edge tends to be a straight line as expected (the length term is enforced). In fact, if we consider equation (5.1) without the fourth order derivatives, the adaptive algorithm gives a solution u that converges to that given by the Mumford-Shah model in the sense of the Γ-convergence [5, 18]. It is well know that the preferable edge curves in the Mumford-Shah model are those which have the shortest length because the penalization term acts on the length of the edge only. Therefore, promoting the second term allows the model to favors straight edges to commit the connectivity principle in perception [20].

Other examples are presented in Fig. 7 and Fig. 9 in order to illustrate the effectiveness of the proposed algorithm for the inpainting of curvature. The curvature in Fig. 7 is well inpainted which proves that our approach, based on fourth order linear diffusion models, allows us to obtain a very interesting result that one might expect by solving some sophisticated models like the Euler's elastica [41], which is highly nonlinear and numerically difficult to solve. We give in Fig. 10 a zoom caption in the damaged region 2 which proves that the missing part is well restored and is very close to the original one.

6.2.2. "Real world"-image inpainting. The experiment in Fig. 11 shows the efficiency of the proposed method in a real image inpainting. The portion of unknown pixels is 45%, 55% and 75%, respectively. From these experiments, we can see that the proposed model can successfully recover the inpainting domain even when up to 75% of pixels are unknown.

6.2.3. Comparison with the Cahn-Hilliard model. In Fig. 12, we have chosen the same image presented by Bertozzi, Esedoglu and Gillette (2006). We give their result which was obtained by solving the Cahn-Hiliard equation and the one obtained using our approach (5.1) for $\alpha = \beta$. We display the evolution of the restored image at iteration 1, 5 and 10 which shows that the edges are progressively and sharply approximated and the four corners are very accurately matched. In fact, the combination of (square) curvature and length terms is the right strategy for such inpainting and restoration problems. The only, difficult, thing to manage in the modeling process is the balance between them. We give an answer to this question with our approach. Notice that the image for Cahn-Hilliard equation (right-hand plot of Fig. 12) is computed in a two steps process. In the first step, the authors solved their equation with a large value of ϵ, e.g., $\epsilon = 0.1$, until the numerical scheme is close to a steady state. In this step, the level lines are continued into the missing domain. In a second step, they used the previous result as an initial time condition u_0 for a smaller ϵ (e.g., $\epsilon = 0.01$) in order to sharpen the contours. This is an adaptive choice for ϵ, however, subjected to a hand tuning and being uniform in the entire domain.

7. Conclusion. In this article, we have investigated some multiscale fourth-order diffusion PDEs for image restoration and inpainting. The continuous models are linear and variational. We introduced an adaptive approximation procedure which is nonlinear, but completely a posteriori strategy, e.g. the selection of the diffusion coefficients is based upon information on the computed solutions during the solution steps. We analyzed our approach from the variational point of view and we established its connections with a Mumford-Shah-like energy, in the sense of the Γ-convergence. We have implemented the considered models to test the method, we have also made some comparisons with existing approaches to demonstrate its capabilities. We have underlined, in the presented tests, the good quality in the recovery of low dimensional sets (edges, corners) and curvature in the inpainted zone. We emphasize that in our approach the adaptive selection of the diffusion coefficients is:

i) Automatic, i.e., no external intervention on the algorithm.
ii) Objective and a posteriori, i.e., the scale of α (the way to decrease its values) is explicitly obtained from computable quantities (error indicators) which are very sensitive to the singularities of the solution.
iii) Local, i.e., at each location in the computation domain (finite-element cell, thus the pixel scale).
iv) Low cost, thanks to the coarsening of the mesh in the homogeneous parts of

the domain.

In addition, the method may be improved straightforwardly by taking α the diffusion function as a matrix which introduces some anisotropy in the models and the overall approach is easy to implement in the framework of variational methods of approximation and remains compatible with most existing variational models.

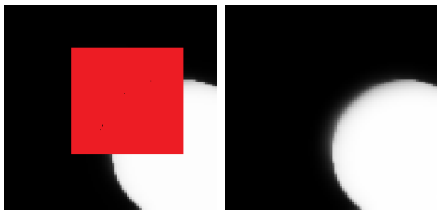

FIG. 4. *Damaged and original images*

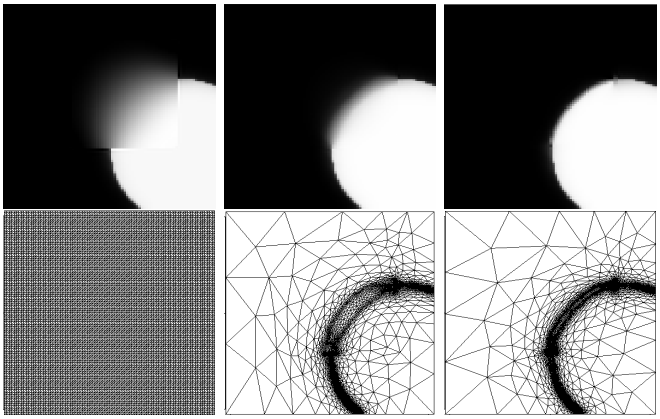

FIG. 5. *Top row: Restored image using the model (1.9) and adaptation at iterations 1, 5 and 20, respectively. Bottom row: Mesh evolution at iterations 1, 5 and 20, respectively*

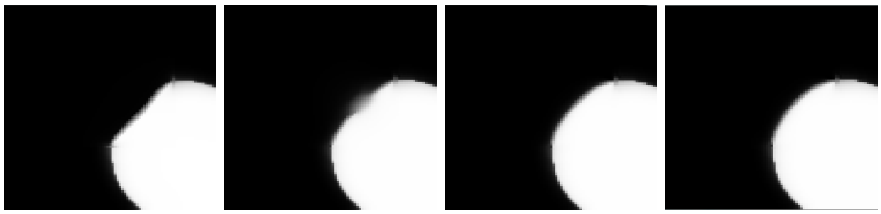

FIG. 6. *Model (5.1) and adaptation: the ratio* $\frac{a}{b} = 0.2, 1, 5$ *and* 10*, respectively.*

REFERENCES

[1] L. AMBROSIO, N. FUSCO, AND D. PALLARA, *Functions of Bounded Variation and Free Discontinuity Problems*, Oxford Mathematical Monographs, 2000.

[2] L. AMBROSIO AND S. MASNOU, *A direct variational approach to a problem arising in image reconstruction*, Interfaces and Free Boundaries, 5 (2003), pp. 63–81.

FIG. 7. *Form left to right: Original, damaged and restored images using model (1.9) and adaptation.*

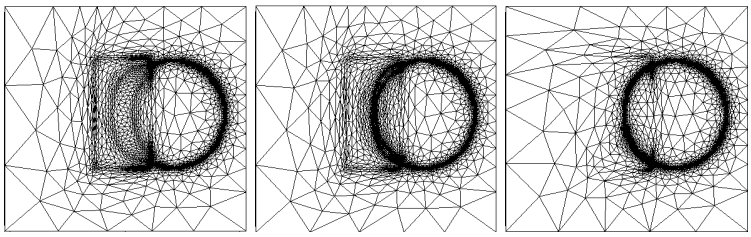

FIG. 8. *Mesh evolution at iterations 2, 5 and 10, respectively.*

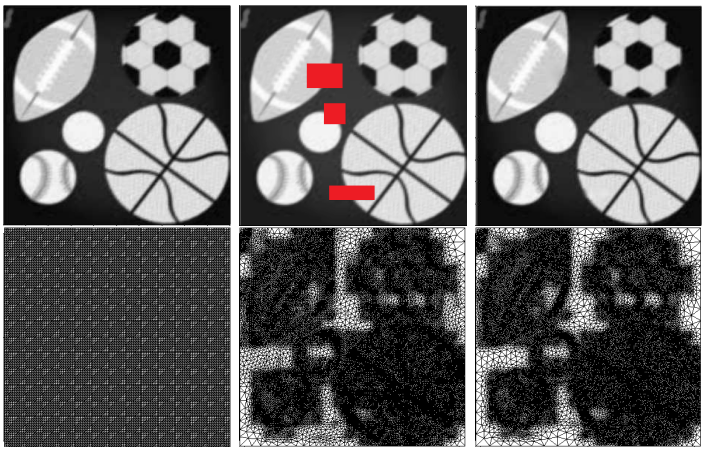

FIG. 9. *Top row: Restored image using model (1.9) and adaptation at iterations 1, 5 and 20, respectively. Bottom row: The evolution of the mesh at iterations 1, 5 and 20, respectively*

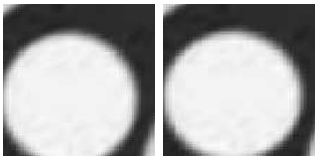

FIG. 10. *Zoom on the damaged region 2: Original and restored.*

[3] L. AMBROSIO AND M. TORTORELLI, *Approximation of functional depending on jumps by elliptic functional via γ-convergence*, Comm. Pure Appl. Math., 43 (1990), pp. 999–1036.
[4] ———, *On the approximation of free discontinuity problems*, Boll. Un. Mat. Ital., 6 (1992), pp. 105–123.

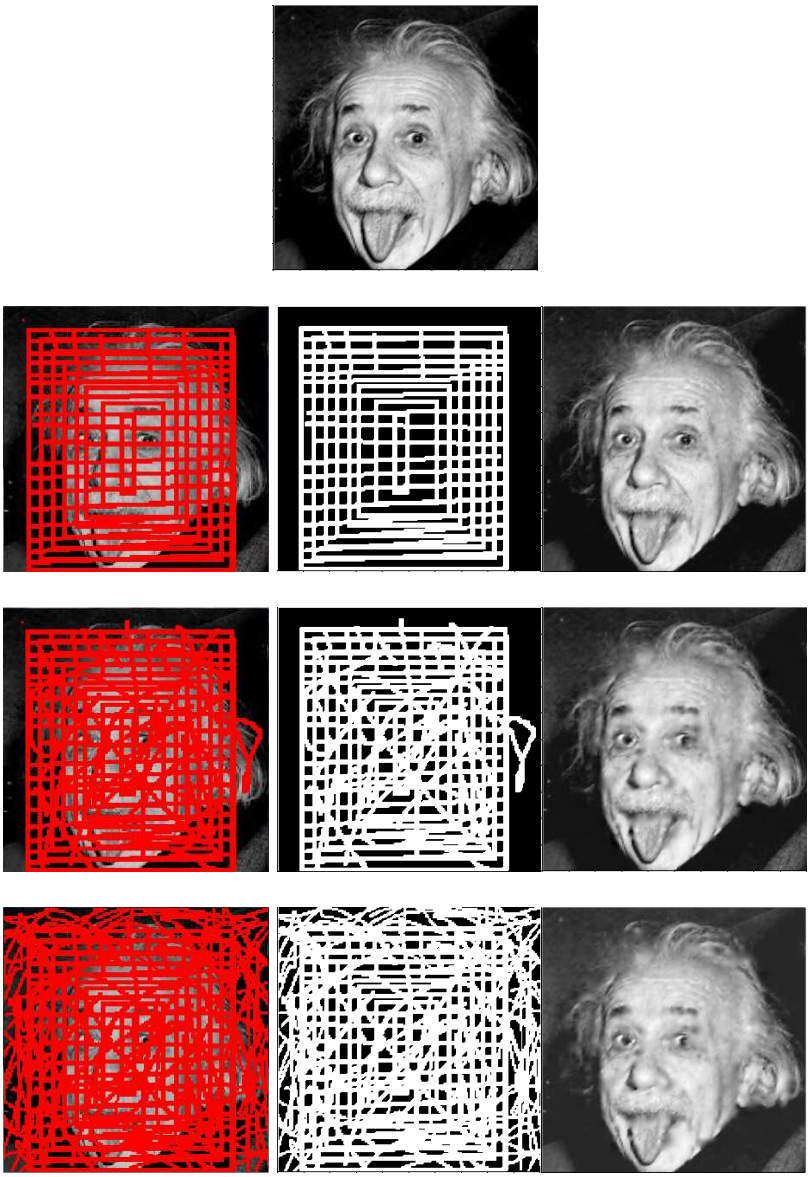

FIG. 11. *The damaged, mask and restored images, respectively. Over:* 45% *of pixels are damaged- Middle:* 55% *of pixels are damaged. Below:* 75% *of pixels are damaged.*

[5] Z. BELHACHMI AND F. HECHT, *An adaptive approach for segmentation and TV edge-enhancement in the optic flow estimation*, Submitted.

[6] ———, *Control of the effects of regularization on variational optic flow computations*, Journal of Mathematical Imaging and Vision, 40 (2011), pp. 1–19.

[7] M. BERTALMIO, A. L. BERTOZZI, AND G. SAPIRO, *Navier-Stokes, fluid dynamics, and image and video inpainting*, in Proceedings of the International Conference on Computer Vision and Pattern Recognition, Hauai, HI, New York, 2001, IEEE, pp. 355–362.

[8] M. BERTALMIO, G. SAPIRO, V. CASELLES, AND C. BALLESTERI, *Image inpainting*, in Proceedings of the 27th annual Conference on Computer Graphics and Interactive Techniques, New York, 2000, ACM, pp. 417–427.

[9] A. BERTOZZI, S. ESEDOGLU, AND A. GILLETTE, *Analysis of a two-scale Cahn-Hilliard model*

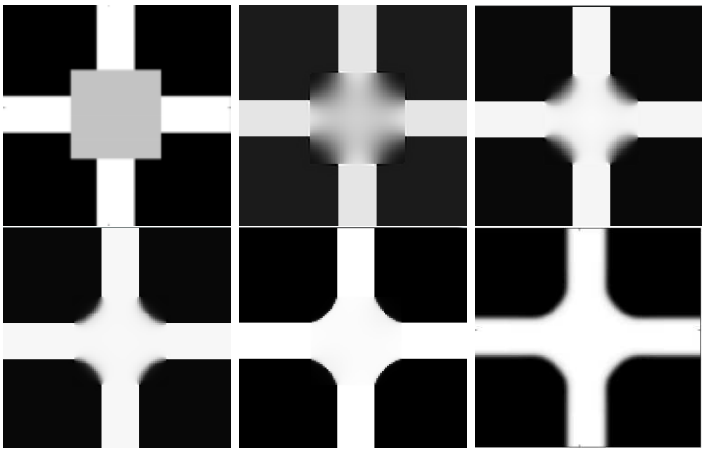

FIG. 12. *Top: Damaged and restored images using model (5.1) and adaption (iterations 1 and 5). Bottom: Restored images using model (5.1) and adaption (iterations 10 and 20) and Cahn-Hilliard (Result obtained by Bertozzi, Esedoglu and Gillette (2007) [10]).*

for image inpainting, Multiscale Modeling and Simulation, 6 (2007), pp. 913–936.
[10] ———, *Inpainting of binary images using the Cahn-Hilliard equation*, IEEE Trans. Image Proc., 16 (2007), pp. 285–291.
[11] A. BERTOZZI AND C.-B SCHONLIEB, *Unconditionally stable schemes for higher order inpainting*, Communications in Mathematical Sciences, 9 (2011), pp. 413–457.
[12] A. BRAIDES, *Gamma-Convergence for Beginners*, vol. 22 of Oxford Lecture Series in Mathematics and its Applications, Oxford University Press, 2002.
[13] C. BRITO-LOEZA AND K. CHEN, *Fast numerical algorithms for Eulers elastica inpainting model*, Int. J. Modern Math., 5 (2010), pp. 157–182.
[14] M. BURGER, L. HE, AND C.-B SCHNLIEB, *Cahn-Hilliard inpainting and a generalization for grayvalue images*, SIAM J. Imaging Sci., 2 (2009), pp. 1129–1167.
[15] J. CAHN AND E. HILLIARD, *Free energy of a nonuniform system. I. Interfacial free energy*, Journal of Chemical Physics, 28 (1958).
[16] A. CHAMBOLLE AND B. BOURDIN, *Implementation of an adaptive finite-element approximation of the Mumford-Shah functional*, Numer. Math., 85 (2000), pp. 609–646.
[17] A. CHAMBOLLE AND P. LIONS, *Image recovery via total variation minimization and related problems*, Numerische Mathematik, 76 (1997), pp. 167–188.
[18] A. CHAMBOLLE AND G. DAL MASO, *Discrete approximation of the Mumford-Shah functional in dimension two*, M2AN Math. Model. Numer. Anal., 33 (1999), pp. 651–672.
[19] T. CHAN AND J. SHEN, *Non-texture inpainting by curvature-driven diffusion (CDD)*, J. Visual Comm. Image Rep., 12 (2001), pp. 436–449.
[20] ———, *Mathematical models for local non-texture inpainting*, SIAM Journal on Applied Mathematics, 62 (2002), pp. 1019–1043.
[21] G. CHUNG, J. HAHN, AND X. TAI, *A fast algorithm for Euler's elastica model using augmented Lagrangian method*, SIAM Journal on Imaging Sciences, 4 (2011), pp. 313–344.
[22] R. DAUTRAY AND J.-L. LIONS, *Mathematical Analysis and Numerical Methods for Science and Technology, Vol. 2, Functional and Variational Methods*, Springer-Verlag, 1988.
[23] S. ESEDOGLU AND J. SHEN, *Digital image inpainting by Mumford-Shah-Euler model*, European Journal of Applied Mathematics, 13 (2002), pp. 353–370.
[24] L. C. EVANS, *Partial Differential Equations*, vol. 19 of Graduate Studies in Mathematics, American Mathematical Society, Providence, Rhode Island, 1998.
[25] E. DE GIORGI, *Frontiere orientate di misura minima*, Sem. Mat. Scuola Norm. Sup. Pisa, (1960).
[26] E. DE GIORGI, *Some remarks on γ-convergence and least squares methods*, in Composite Media and Homogenization Theory, G. Dal Maso and G. F. Dell'Antonio, eds., Birkhauser Boston, Cambridge, MA, (1991), pp. 135–142.
[27] F. HECHT, *New development in freefem++*, Journal of Numerical Mathematics, 20 (2002), pp. 251–265.

[28] W. Hinterberger and O. Scherzer, *Variational methods on the space of functions of bounded Hessian for convexification and denoising*, Computing, 76 (2006), pp. 109–133.
[29] M. Kallel, M. Moakher, and A. Theljani, *The Cauchy problem for a nonlinear elliptic equation: Nash-game approach and application to image inpainting*, Submitted to: Inverse Problems and Imaging, (2014).
[30] H. Linh and L. Vese, *Image restoration and decomposition via bounded total variation and negative Hilbert-Sobolev spaces*, Appl. Math. Optim., (2008), pp. 167–193.
[31] M. Lysaker, A. Lundervold, and X. C. Tai, *Noise removal using fourth-order partial differential equation with applications to medical magnetic resonance images in space and time*, IEEE Transactions on Image Processing, 12 (2003), pp. 1579–1590.
[32] M. Lysaker and X. C. Tai, *Iterative image restoration combining total variation minimization and a second-order functional.*, International Journal of Computer Vision, 66 (2006), pp. 5–18.
[33] S. Masnou, *Filtrage et désocclusion d'images par méthodes d'ensembles de niveau*, PhD thesis, Université Paris-Dauphine, 1998.
[34] S. Masnou, *Disocclusion a variational approach using level lines*, IEEE Transactions on Image Processing, 11 (2002), pp. 68–67.
[35] S. Masnou and J. M. Morel, *Level-lines based disocculusion*, Proceedings of 5th IEEE International Conference on Image Processing, (1998), pp. 259–264.
[36] M. Nitzberg, D. Mumford, and T. Shiota, *Filtering, segmentation and depth*, volume 662 of Lecture Notes in Computer Science. Springer, (1993).
[37] S. Osher, A. Sole, and L. Vese, *Image decomposition and restoration using total variation minimization and the H^{-1} norm*, Multiscale Model. Simul., 1 (2003), pp. 349–370.
[38] K. Papafitsoros and C.-B Schonlieb, *A combined first and second order variational approach for image reconstruction*, Journal of Mathematical Imaging and Vision, 48 (2014), pp. 308–338.
[39] L. I. Rudin, S. Osher, and E. Fatemi, *Nonlinear total variation based noise removal algorithms*, Physica D: Nonlinear Phenomena, 60 (1992), pp. 259–268.
[40] O. Scherzer, *Denoising with higher order derivatives of bounded variation and an application to parameter estimation*, Computing, 60 (1998), pp. 1–27.
[41] J. Shen, S. H. Kang, and T. Chan, *Euler's elastica and curvature-based inpainting*, SIAM J. Imaging Sci., 63 (2002), pp. 564–592.
[42] A. Tikhonov and V. Arsenine, *Méthodes de Résolution de Problèmes Mal Posés*, Mir, Moscou, 1977.